Spectral Imaging of the Retina

Andy R Harvey†, Ied Abboud, Alistair Gorman, Andy McNaught*, Sonny Ramachandran and Eirini Theofanidou

School of Engineering and Physical Sciences, Heriot Watt University, Edinburgh, EH14 4AS, UK
†e-mail a.r.harvey@hw.ac.uk
*Cheltenham General Hospital, Department of Ophthalmology, Sandford Rd, Cheltenham, GL53 7AN, UK

ABSTRACT

Spectral imaging of the retina shows great promise for the early detection of retinal disease through retinal screening programs. Implementation of such a program will require instrumentation capable of efficiently recording the requisite spectral data cube. We report on the development of two candidate approaches: one employs a traditional liquid crystal tunable filter to filter the illumination source and enable the spectral data cube to be assembled from mutually coregistered narrow-band images recorded in time sequence; the second employs, IRIS, a novel image replicating imaging spectrometer to record a two-dimensional spectral data cube in a single snapshot.

INTRODUCTION

Spectral imaging involves the recording of a spectrum for each pixel within a scene. The spectral data set is therefore referred to as a spectral data cube where two dimensions are the conventional transverse image co-ordinates and the third dimension is wavelength. Since the raw image data is captured using a two-dimensional detector array, at least one of these dimensions has to be obtained by some form of multiplexing of the captured data onto a two-dimensional data cube[1]. This normally means that a snapshot is recorded in two of the dimensions and the third dimension is scanned in time sequence. For direct imaging this involves either (a) images of a scene are recorded in time sequence as narrow-band light illuminating or reflected from the scene is scanned in wavelength or (b) a one-dimensional line is dispersed onto a two-dimensional detector enabling a one-dimensional spectral image to be recorded in a snapshot; a three dimensional spectral image is assembled by scanning the footprint of the one-dimensional image across one of the transverse dimensions of the scene. Fourier-transform spectral imaging equivalents of method (a) are achieved by imaging the scene through a time-sequentially scanned interferometer (typically a Michelson interferometers, although birefringent interferometers may also be used[2]). The Fourier-transform equivalent of method (b) is achieved with a one-dimensional imaging static Fourier-transform spectrometer[3].

For spectral imaging of the retina, the most appropriate technique depends on the objective. The use of one-dimensional spectral imaging offers the very important advantage that it enables a spectral image, albeit a spectral image of only a single line, to be recorded in a single snapshot[4]. This means that the spectral distortion that can be introduced by misregistration of time-sequential narrowband images is absent. The resultant one-dimensional spectral images may be located so as to intersect points of interest on the retina, such as a blood vessel, thereby enabling blood oximetry. The major disadvantage of this technique appears to be that it does not provide an extended two-dimensional field of view as clinicians desire for screening for retinal disease. It is therefore less well suited to a routine retinal screening program. In contrast, we have chosen to record time-sequential spectral images of the retina that are coregistered in software to produce a two-dimensional spectral image of the retina. This offers the advantage of a two-dimensional wide field-of-view as is desirable for routine screening. It also allows the additional possibility of recording a reduced set of narrow-band images only at a set of wavebands for which the most useful spectral information exists. The number of images that need to be recorded to produce a spectral image of the retina can therefore be the minimum necessary. Furthermore, in contrast to Fourier-transform spectral imaging and spectral imaging where the light is filtered between the eye and the detector, the light is filtered before illuminating the retina so the light intensity at the retina, and the associated discomfort for the patient, is minimised. There are, however, additional problems introduced by this approach associated with the need to co-register the narrowband images and to calibrate the effects of varying retinal illumination between images. These issues are described here. We also describe the application of a novel technique called image replication

imaging spectrometry that combines the benefit of spectral imaging in two dimensions with the simplified calibration and coregistration of snapshot spectral imaging.

TIME SEQUENTIAL IMAGING SPECTROMETRY

To enable time-sequential spectral imaging, we have incorporated a liquid crystal tuneable filter (LCTF) into the illumination path of a commercial fundus imager. The filtered light at the retina is significantly reduced in intensity compared to the unmodified camera and this has necessitated the use of a low-noise cooled CCD camera. Flash illumination can be varied in intensity by a factor of more than one hundred to compensate for the spectrally varying illumination intensity and transmission of the eye-instrument system. This enables the full dynamic range of the detector to be exploited; a feature that is not possible with other spectral imaging modalities. In this system the number of photoelectrons detected can be typically 10^4 or greater per pixel per image and the dominant noise source across most of the spectral band is photon-shot noise. The flash and camera data acquisition are synchronized and controlled by a computer under *Labview* software.

The unmodified fundus camera incorporates some small axial masks in the illumination path that prevent the excitation of reflections from the two surfaces of the objective lens of the fundus camera. This lens is a field lens and so is conjugate with the retina so that reflections from its surface can cause high-intensity artifacts in the retinal image. The additional optical path introduced by the LCTF necessitates careful relocation of these axial masks.

The fundus camera used is a Canon CR4, which is designed to be used with mydriasis and has a flash recycle rate of faster than 1 Hz. When used for spectral imaging, this enables a spectral data cube covering the most useful range of 400-720 nm to be recorded at 10 nm resolution in less than one minute.

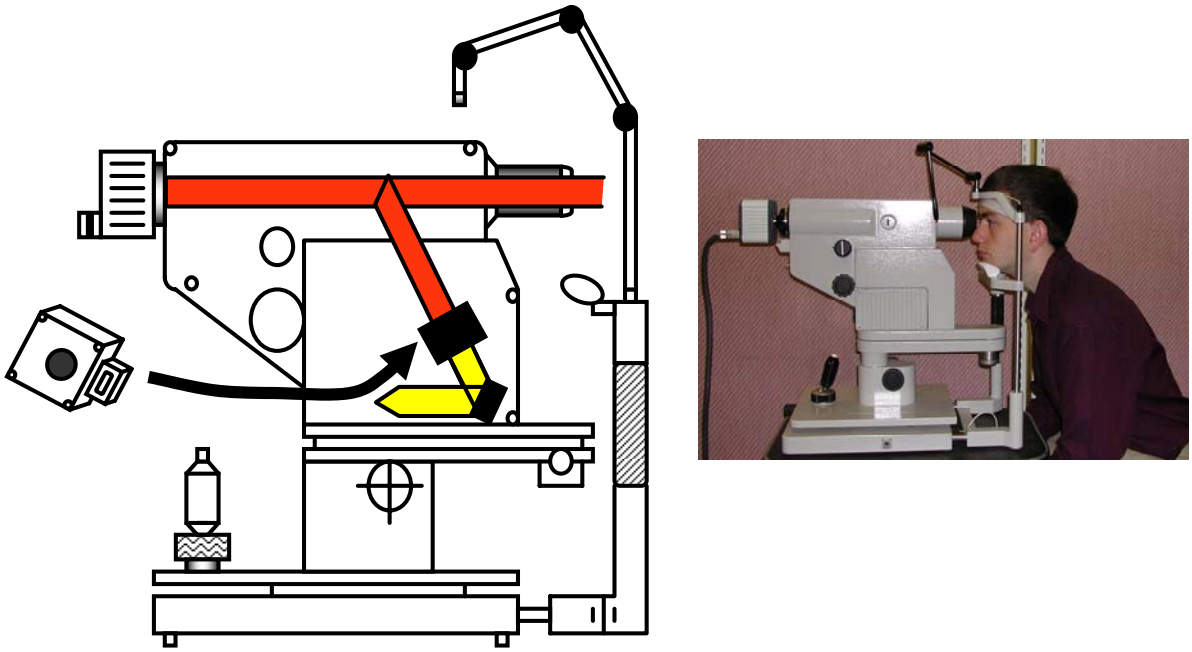

Figure 1 Hyperspectral retinal fundus camera showing the location of the LCTF in the illumination beam.

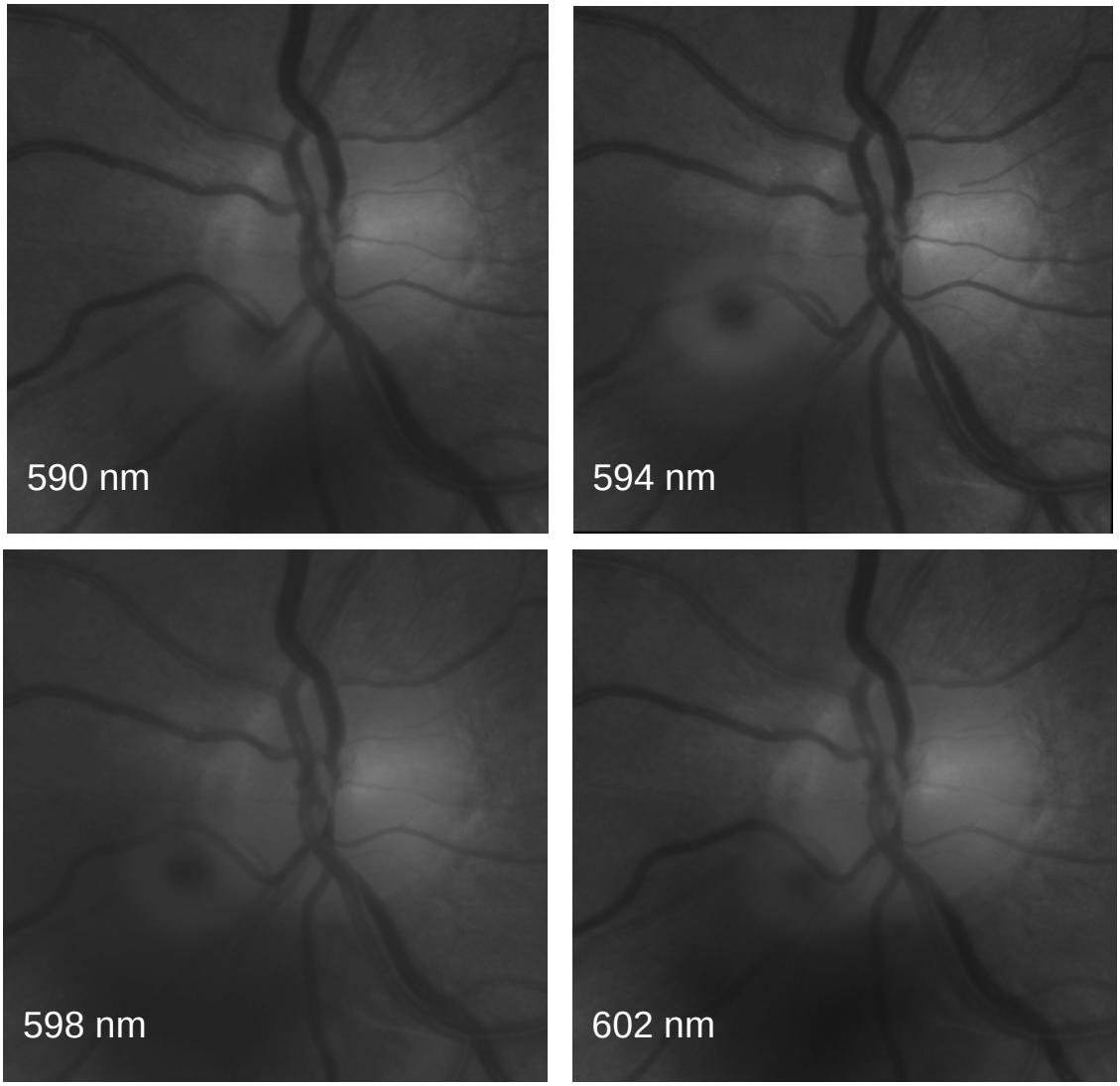

Figure 2 Images of the optic disk at wavelengths where oxygenated blood arteries undergo a rapid transition from opaque to transparent.

Narrow-band spectral images are mutually coregistered to correct for rotational and translational offsets introduced by movement of the eye between images. A relatively simple cross-correlation technique has been found to enable accurate coregistration. Prior to cross-correlation, images are spatially filtered to enhance blood vessels since these serve as good spectrally invariant landmarks. Filtering consists of the following steps which were optimized heuristically: bandpass filtering, matched filtering and edge detection. Using a single set of filtering parameters it is possible to reliably co-register images for wavelengths between 420 and 840 nm. During recording, patients are asked to fixate on an LED so as to reduce movement of the eye. The resulting calculated root-mean-squared mutual offsets between retinal images are typically about 1º in translation and about 0.3º in rotation.

A typical set of images taken from a spectral data cube is shown in Figure 2 for wavelengths between 590 nm and 602 nm. This corresponds to the wavelength range for which the optical depth of oxygenated haemoglobin changes from being less than, to being greater than, the thickness of the larger retinal arteries. As can be seen in the images, the larger arteries change from being almost opaque to highly transparent across this spectral range so that it is possible to determine blood oxygenation from the change in optical density of blood in this wavelength region. From inspection of

the data cube from which the images of Figure 2 were taken one can conclude that the mutual coregistration of these images cannot be improved upon insomuch as the image-to-image overall misregistration between retinal structures appears to be minimised. Some misregistration remains, however, due to differential distortion of the retina for differential synchronisations of the image recording times with the heart pulse. This is illustrated by the image on the right, which shows the intensity ratio of two consecutive images recorded at a wavelength of 580nm. The highlighting of the blood vessels and predominantly the arteries is due to pulse-induced distortion. Synchronisation of the data acquisition with the pulse will reduce this effect; however, artefacts due to non uniform illumination of the retina and due to differential imaging distortion will remain. This in turn introduces errors in the calculated spectra. The time sequential imaging technique described below does not suffer from these effects and furthermore is able to record time-resolved spectral signatures.

Figure 3 Depiction of image retinal motion between nominally identical frames

SNAPSHOT SPECTRAL IMAGING IN TWO-DIMENSIONS

The flexibility of the time-sequential imaging technique outlined above is highly suited to researching the spectral signatures of the eye, but for clinical applications and for improved accuracy and clinical convenience, the image replication imaging spectrometer (IRIS)[5,6] described in this section, offers the advantage of recording a complete spectral image in a single snapshot. IRIS can be considered as a generalisation of a Lyot filter, which enables high efficiency spectral demultiplexing of broadband light. The Lyot filter[7,8,9,10], as used for many years in astronomy, employs polarising interferometry within multiple waveplates to yield a narrow-band filter suitable for recording monochromatic images. Light not transmitted by the Lyot filter is absorbed by film polarisers. To generalise the Lyot filter, Wollaston prism polarising beam splitters are used in place of film polarizers enabling spectral images to be recorded simultaneously in several pass-bands without rejection of light. To describe the principle of operation of IRIS we will first consider the principle of a conventional Lyot filter.

A Lyot filter, as illustrated in Figure 4, is composed of multiple waveplates sandwiched between co-aligned linear polarisers aligned to pass light polarised at 45º to the fast axis of each waveplate. The linearly polarised light propagating through the waveplate is resolved into orthogonally polarised components that interfere at the output analysing polariser with a mutual optical path difference $(n_o-n_e)t$ between the orthogonal components where n_o and n_e are the ordinary and extraordinary refractive indices of the waveplate and t is its thickness. The output polariser is aligned with the input polariser so that the overall transmission function of the polariser-waveplate-polariser assembly is proportional to $\cos^2(\pi\nu(n_o-n_e)t)$ where $\nu=1/\lambda$ is optical frequency. A Lyot filter consists of an assembly of multiple polariser/waveplate combinations where the ratio between the thicknesses of consecutive waveplates is a factor of two. The spectral transmission function of an n-waveplate Lyot filter is thus the product of the transmission functions of all constituent waveplate/polariser assembly and is given by

$$T(\nu)=\prod_{i=1}^{n}\cos^2\left(i\pi\nu\left(n_o-n_e\right)t_i\right) \tag{1}$$

where t_i is the thickness of waveplate *i*. A generalisation of this technique is employed with the IRIS concept described here whereby the film polarisers are replaced with Wollaston prism polarising beam splitters as shown in Figure 5. The use of a polarising beam splitter means that after transmission through each waveplate the light is resolved into polarisations both, aligned with, and orthogonal to, the input polarisation state. As with the Lyot filter, for the co-polarised component the transmission function is given by $\cos^2(\pi\nu(n_o-n_e)t)$; for the cross-polarised component the transmission function is $\sin^2(\pi\nu(n_o-n_e)t)$. Furthermore, these two orthogonally polarised components are displaced in angle by the beam-splitting action of the Wollaston prism and this enables two spatially separated and spectrally filtered replica images to be formed. Subsequent Wollaston prism polariser pairs further spectrally filter and replicate the images. After transmission through *n* Wollaston prism polariser pairs, 2^n replicated images are formed, each with a unique product of $\sin^2$and $\cos^2$ transmission functions. It can be seen then that the IRIS technique simultaneously replicates the image formed at the field stop whilst applying a unique spectral filtering function to each image; this filtering function is determined by how light arriving at each image was steered and spectrally modulated. IRIS thus performs the function of an imaging spectral demultiplexor with image components lying within a spectral band tending to be steered to a particular part of the detector array. The images at the detector array are prevented from overlapping by the field stop.

The orientation and magnitude of the splitting angles of the splitting angles of the Wollaston prisms determine the locations of the replicated images at the detector; each image can be identified by a vector {$p(1)$, $p(2)$.. $p(n)$} where each element of the vector identifies whether the image is due to refraction in a positive or negative direction at each Wollaston prism. In general, the transmission function for each image at location {$p(1)$, $p(2)$.. $p(n)$} in the image plane can be written as

$$T_{p(1),p(2)..p(n)}(\nu)=\prod_{i=1}^{n}\Omega_{a(n)}\left(i\pi\nu b(\nu)t_i\right) \tag{2}$$

Where $b(\nu)=n_o(\nu)-n_e(\nu)$, $a(i)$ refers to either co-polar or cross-polar transmission between Wollaston prisms, so that the respective transmission functions for co-polar and cross-polar transmissions through waveplate *i* sandwiched between polarisers *i*-1 and *i* are

$$\Omega_{a(i)=co-polar}(x)=\cos^2(x) \tag{3}$$

$$\Omega_{a(i)=cross-polar}(x)=\sin^2(x) \tag{4}$$

where suffix i=0 indicates the input polarizer and all other values indicate Wollaston prism polarizers. The spectrum associated with each individual image replication is determined by the vector {$a(1)$, $a(2)$,.. $a(n)$} appropriate for each image replication. Since spectral filtering and image replication operations commute, the order of the vector elements is not important; it will always result in the same combination of 2^n products of the *n* pairs of $\cos^2$ and $\sin^2$ functions being applied at the image. Due to the wide spectral range of IRIS it is necessary to use the dispersive variation of $b(\nu)$ with wavenumber when evaluating (2). The resultant pass-bands are bell-shaped and exhibit significant sidelobes. The presence of sidelobes mean that the spectral transmission functions are non-orthogonal and hence this results in some reduction in the separation of spectra in spectral space. Optimisation of the waveplate thicknesses *t* yields a significant reduction in sidelobe level such that the separation in spectral space can be greater than 95% of that that would be obtained with orthogonal functions.

For visible band imaging, quartz is an ideal material for the waveplates since its relatively small birefringence yields relatively thick and robust waveplates with relaxed manufacturing tolerances. An IRIS system was designed and manufactured with three waveplates and Wollaston prisms to produce eight narrow-band images with centre wavelengths in the range 575 to 615 nm. The measured transmission of this assembly is shown in Figure 6. The spectral

transmission is restricted by low-pass and high-pass edge filters. The total transmission efficiency of only the birefringent components, obtained by summing the transmissions into each spectral band, is a minimum of 95% across the full spectral transmission width. The IRIS system is assembled as shown in Figure 8 and a photograph of only the birefringent components is shown in Figure 9.

As a proof of principle, this IRIS system was used to replicate and spectrally demultiplex the image at the output port of a conventional fundus camera; an example recorded image is shown in Figure 9. After correction of imaging distortion, these images have been decomposed into their constituent eight images and have been mutually coregistered, prior to spectral processing. The results of a principle components analysis are shown in Figure 9, where PC1 appears to be anti-correlated with the spectrum of both oxygenated and deoxygenated hemoglobin and PC2 appears to be correlated with oxygenated hemoglobin. Further work is required to process these recorded images to yield estimates of blood oxygenation.

CONCLUSIONS

We report two techniques that are being developed for spectral imaging of the retina. The first, based on time-sequential spectral imaging, offers the combined advantages of imaging a two-dimensional image of the retina with flexible selection of wavelength bands. It is however subject to some artifacts associated with the time-sequential nature; techniques for the mitigation of these artifacts are currently being researched. This technique is particularly suitable for clinical research, but for clinical application, the two-dimensional snapshot capability of IRIS constitutes a major advantage. In its current embodiment this has fixed wavelength bands and so the optimum wavelength bands selected depend upon the application. Thus the two techniques described are mutually complementary: the time-sequential spectral imaging technique enables the optimum wavebands to be determined and this informs the design of a high-performance, snapshot spectral retinal camera based on IRIS.

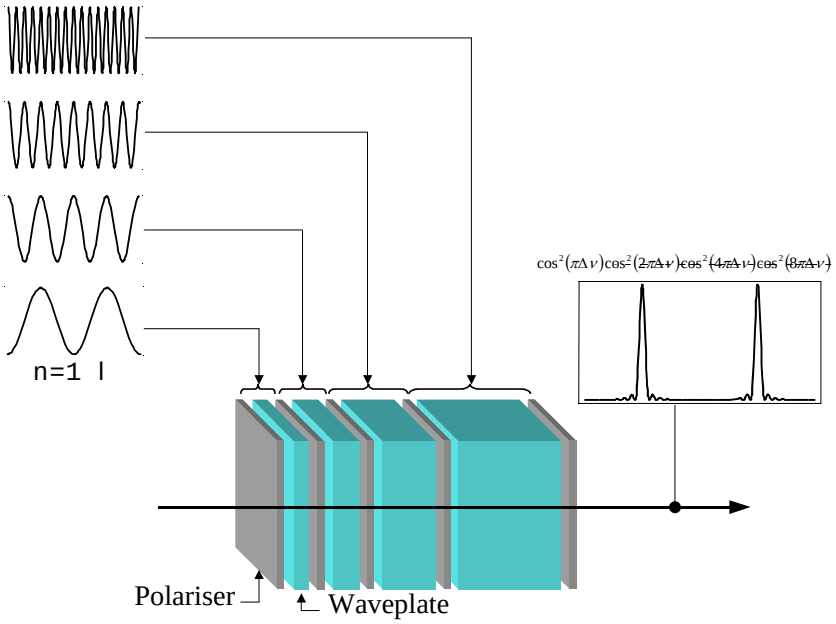

Figure 4 Depiction of the principle of operation of the Lyot filter

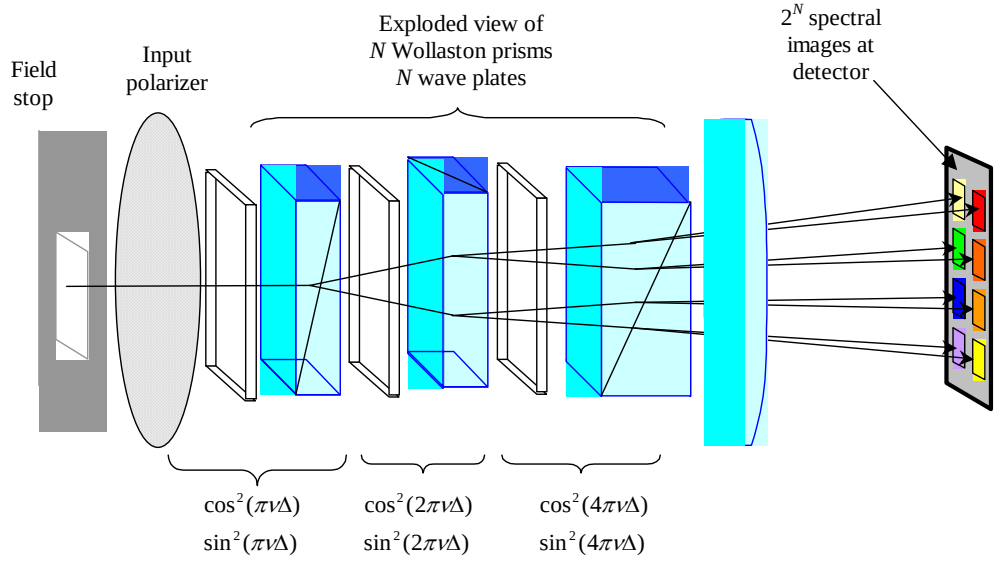

Figure 5 Depiction of the Image Replicating Imaging Spectrometer

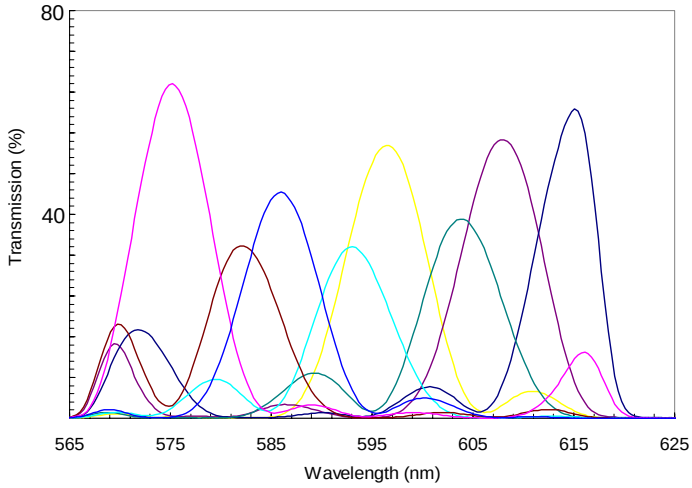

Figure 6 Spectral passbands for retinal blood oximetry

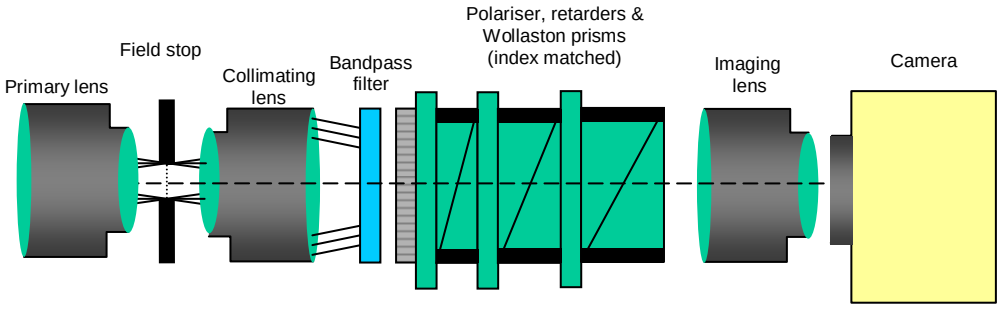

Figure 7 Schematic of the implementation of the 8-channel IRIS concept within a spectral imager

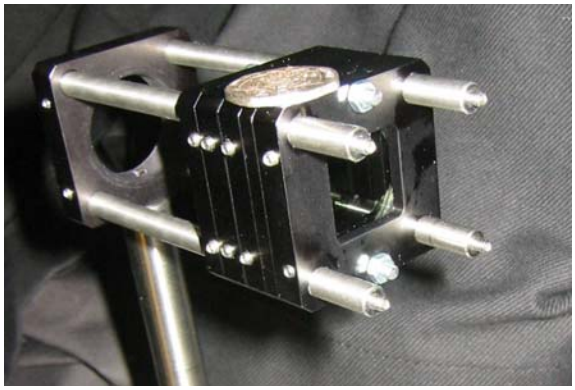

Figure 8 Assembled Wollaston prisms and waveplates for an 8-channel IRIS

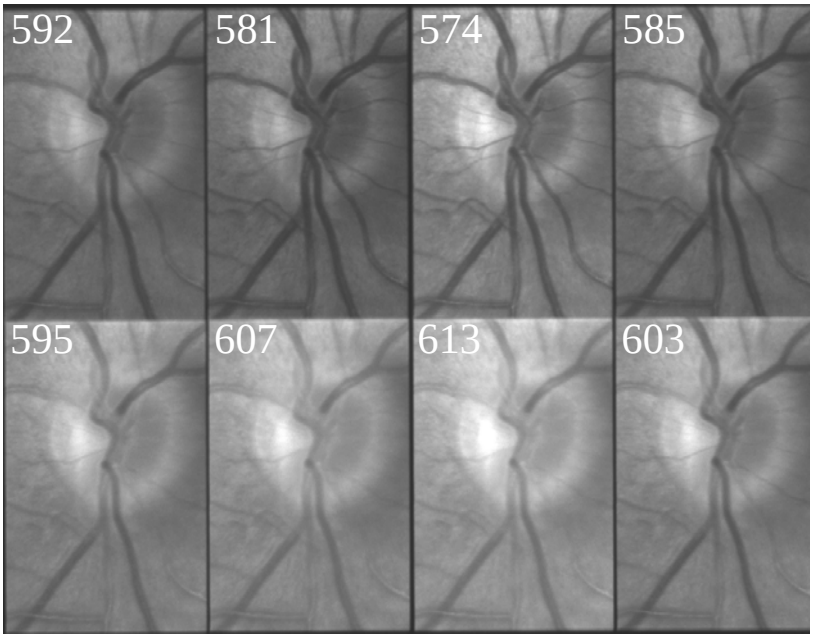

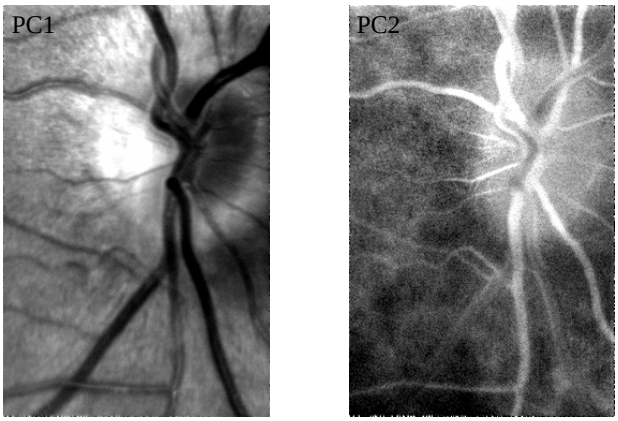

Figure 9 Image replicated narrow-band images as recorded by the detector (left) and after principle component analysis (right)

REFERENCES

[1] A.R. Harvey, J. Beale, A.H. Greenaway, T.J. Hanlon and J. Williams, "Technology options for imaging spectrometry" *Proc SPIE*, 4132, pp13-24, 2000

[2] A R Harvey, D W Fletcher-Holmes, *Birefringent Fourier-transform imaging spectrometer*, Optics Express **12**, 22, pp 5368-74, (2004)

[3] P W Truitt, P Soliz, A D Meigs, L J Otten, Hyperspectral fundus imager, Imaging Spectrometry VI, SPIE 4132, pp 356-364 (2000)

[4] M Hammer, D Schweitzer, L Leistritz, M Scibor,K Donnerhacke,‡ and J Strobel, *Imaging spectroscopy of the human ocular fundus in vivo*, journal of biomedical optics 2(4), 418–425 (1997)

[5] A R Harvey, D.W. Fletcher-Holmes, *Imaging Apparatus*, Patent WO2004 005870 A1, (2004)

[6] A R Harvey, D. W. Fletcher-Holmes, A. Gorman, K. Altenbach, J. Arlt, N. D. Read, *Spectral imaging in a snapshot*, Spectral Imaging: Instrumentation, Applications, and Analysis III, Proc. SPIE Vol. 5694, p. 110-119, (2005)

[7] B. Lyot, *Filter monochromatique polarisant et ses applications en physique solaire*, Ann. Astrophys. 7, 32 (1944)

[8] B. Lyot, *Optical apparatus with wide field using interference of polarized light*, C.R. Acad. Sci. (Paris) 197, 1593 (1933).

[9] Y. Ohman, *A new monochromator*, Nature 41, 157, 291 (1938).

[10] Y. Ohman, *On some new birefringent filter for solar research*, Ark. Astron. 2, 165 (1958).